

GIS-based gully erosion susceptibility modeling, adapting bivariate statistical method and AHP approach in Gombe town and environs Northeast Nigeria

Ogbonnaya Igwe

University of Nigeria

Ikechukwu John Ugwuoke (✉ john.ikechukwu.pg87197@unn.edu.ng)

University of Nigeria <https://orcid.org/0000-0003-0261-2900>

Onwuka Solomon

University of Nigeria

Ozioko Obinna

University of Nigeria

Research

Keywords: GESM, GIS, Prediction, Frequency ratio, Analytical hierarchy process

Posted Date: September 18th, 2020

DOI: <https://doi.org/10.21203/rs.3.rs-30110/v3>

License: © ⓘ This work is licensed under a Creative Commons Attribution 4.0 International License. [Read Full License](#)

Version of Record: A version of this preprint was published on November 23rd, 2020. See the published version at <https://doi.org/10.1186/s40677-020-00166-8>.

Abstract

Gully erosion is a major environmental problem in Gombe town, a large area of land is becoming unsuitable for human settlement, hence the need for a gully erosion susceptibility map of the study area. To generate a gully inventory map, a detailed field exercise was carried out, during this investigation one hundred gullies were identified and studied extensively within the study area of about 550 km². In addition to the mapped gullies, Google EarthPro with high-resolution imagery was used to locate the spatial extents of fifty (50) more gullies. Ten gully erosion predisposing factors were carefully selected considering the information obtained from literature, and multiple field survey of the study area, the factors include elevation, slope angle, curvature, aspect, topographic wetness index (TWI), soil texture, geology, drainage buffer, road buffer and landuse. In this study, a GIS-based Frequency Ratio (FR) and Analytical Hierarchy Process (AHP) models were employed to predict areas prone to gully erosion in Gombe town and environs. The result obtained from FR shows that drainage, soil texture, and slope have the highest correlation with gully occurrence, while the AHP model revealed that drainage buffer, soil texture, geology have a high correlation with the formation of a gully. Gully erosion susceptibility maps (GESM) were produced and reclassified into very high, high, moderate, and low zones. The overall accuracies of both models were tested utilizing area under the curve (AUC) values and gully density distribution. FR and AHP model have AUC values of 0.73 and 0.72 respectively, the outcome indicates that both models have high prediction accuracy. The gully erosion density distribution values revealed that gullies are concentrated in the very high susceptibility class and it decreases towards the low class, therefore the GESM produced using these models in this study area is reliable and can be used for land management and future planning.

Introduction

One of the factors that endanger water and soil is soil erosion (Magliulo, 2012). The major cause of land degradation around the world is soil erosion by gully erosion (Nampak *et al.*, 2018 ;) (Rizeei, H. M *et al* 2016). Gully erosion is defined as a deep channel that is formed by concentrated water flow, which in the process removes surface soils and materials. (Kirkby MJ, Bracken LJ., 2009). The changes in the quantity of moisture content resulting from dry and wet seasons are a major factor contributing to cracks and grooves in clay formations consequently forming rilled erosion and gullies (Torri *et al.*, 2012). Runoff accumulates within these cracks at the first sudden rainfall and consequently, gully develops. Under natural conditions, vegetation helps to hold soil in place and protect it from the direct impact of rainfall thereby controlling run-off. The effect caused by excessive clearing, inappropriate landuse, and compaction of the soil caused by grazing is that the soil becomes exposed and unable to absorb excess water, this implies that there becomes an elevated level of Surface run-off that concentrates in drainage lines, making it possible for the occurrence of gullies in susceptible areas, (Ligonja and Shrestha, 2015). The threat of gully erosion on the socio-economic development of Gombe state (fig.2) includes the destruction of houses, loss of lives, displacement of people, land depreciation, destruction of roads and culverts (Mbaya, 2017). To better identify areas prone to gully erosion and realize the mechanism involved it becomes expedient to invent a gully erosion susceptibility map (GESM) (Arabameri *et al.*, 2018). The demarcation of an area into zones of varying susceptibility is made possible by the estimation of the input of each conditioning factor. Several models have been created and employed to analyze both quantitatively and qualitatively, the rate of gully erosion. Lately, researchers have executed statistical and machine learning methods in other to determine the statistical relationship that exists between gully erosion factors and the spatial distribution of gullies (Magliulo, 2012). Several researchers have assessed control measures and the effect of gully erosion in Gombe town, but no work has been done to produce a reliable gully erosion susceptibility map (GESM) adapting Frequency Ratio (FR) and Analytical Hierarchy Process (AHP) models. The objective of this research includes: To develop a gully inventory map of the study area, secondly, to produce all relevant thematic maps for the conditioning factors and establish the correlation between predisposing factors and gully occurrence, to apply Frequency Ratio and Analytical Hierarchy Process (AHP) models to produce GESM and finally, to validate the produced susceptibility maps using AUC and gully density distribution.

Climate and vegetation

The area is characterized by wet and dry seasons, having a mean annual rainfall and temperature of 850mm and 32°C respectively. Rainfall within the study area occurs mostly between June and September. Precipitation is associated with a storm of high intensity, especially in July and August. The vegetation of the Gombe area can be described as Sudan savannah with open grassland and shrubs which dries up during the dry season, the vegetation comprises of scattered shrubs and trees.

Geology

The study area is located in the north-south trending Gongola basin of the upper Benue Trough, it is underlain by four geologic Formations, they include, Yolde Formation, Pindiga Formation, Gombe Sandstone, and Kerri-Kerri Formation. (fig.2) The Yolde Formation is Cenomanian in age, deposited in continental to the marine environment it comprises of sandstone and shale at the base while the top consists of sandstones, shales, and calcareous sandstone (Abubakar, M. B., *et al.*, 2008). The Cenomanian-Santonian marine Pindiga Formation, consisting of thick marine shale, with some limestone beds toward the base (Zaborski *et al.*, 1997). while the Gombe sandstone is the last cretaceous deposit in the Gongola arm of the Upper Benue trough. It is underlain by the marine Pindiga Formation and overlain by the Kerri-Kerri Formation. The lacustrine to deltaic Gombe Formation consists of well-bedded fine to medium-grained friable, ferruginous sandstone, siltstone, and shale with ironstone (Orazulike, 1987). Three major lithofacies characterize this formation, they include the basal transitional portion, bedded facies, and red sandstone facies. At its base, it comprises intercalation of silty shale occasionally, with plant remains (Zaborski *et al.*, 1997). The continental Kerri-Kerri Formation ended sediment deposition in the Upper Benue Trough; it consists of sandstones, siltstones, and shales.

Geomorphology

The complex geologic crystalline bedrock formed the base on which the relief of Gombe was established. The elevation of the study area is within 330m to 721m (Fig.1). The flat-topped to conical hills characterized the landscape; this landscape is the outcome of dissection and stream incision in the area after the deposition of sedimentary formation during the late cretaceous period. Aside from the Gombe hill and Liji hill (fig.3.) Gombe town is generally taken to be a flat area (Arabi *et al.*, 2009),

Methodology

The methodology employed in this research is summarized in the flowchart in fig.4. The first approach to this study to generate a reliable gully inventory map was to embark on a detailed field survey. Ten gully erosion predisposing factors were carefully selected considering information obtained from the literature and field survey of the study area. Next was to produce thematic maps corresponding with the chosen conditioning factors. ASTER DEM with a resolution of 30m x 30m was used to extract Topographic related factors such as elevation, slope angle, curvature, aspect, topographic wetness index. The geological map was digitized from a previously existing geological map produced by Nigeria Geological Survey Agency (NGSA) while soil map obtained from the Institute for Agricultural Research; Ahmadu Bello University Zaria Nigeria was obtained and digitized to produce the soil texture map of the area. Drainage buffer and road buffer were digitized from Google Earth imagery while Landsat 8TM 30m resolution was employed to produce the landuse map in ArcGIS version 10.4.

The modeling phase required that all the gully erosion training (75%) and testing (25%) data were selected randomly and overlain over all the produced thematic maps in the ArcGIS environment. After the rasterization of all produced thematic maps, in order to ensure uniformity of the areal extent and resolution, the thematic maps were masked with Digital Elevation Model (DEM) of a 30mx30m grid size. The prediction rate acquired from the Frequency Ratio approach together with the criteria weights from the AHP were subsequently integrated into the ArcGIS raster calculator, at this point each conditioning factor map was multiplied with their respective prediction rates and criteria weights, at the end of these process the susceptibility index map was produced. The Gully Erosion Susceptibility Index Maps generated were reclassified into four zones of different degrees of susceptibility to gully occurrence. To validate the accuracy of the

prediction, the area under the curve (AUC) and gully density distribution technique was used. The area of gully erosions in a susceptibility zone was divided by the area of the zone to determine the gully erosion density distribution

Frequency ratio (FR)

Frequency ratio (FR) is the ratio of the area where gullies occurred in the study area to the whole study area. For a given factor, it is the ratio of the possibility of gully occurrence to its nonoccurrence (Lee and Talib 2005). The frequency ratio model is a bivariate statistical method (Ouyang *et al.* 2017) employed for calculating the possible relationship between gully erosion and conditioning factors. It is necessary to have several independent variables that are required to determine the dependent variables (Abedini *et al.* 2017). According to (Oh *et al.* 2017),

$$FR = (A/B) / (C/D)$$

A represents the number of pixels within gully erosion for each class of geo-environmental factors, and B represents the total number of gullies in the study area, while C represents the total number of pixels within each class of the predisposing factors, and finally, D represents the total number of pixels in the study area.

The Frequency Ratio correlation value varies between <1 to >1. When FR value is observed to be less than 1, it indicates a low correlation between gully location and each class of the predisposing factor, on the other hand, a higher correlation exists if the FR value is observed to be higher than 1 (Poudya *et al.* 2010).

Analytic Hierarchy Process (AHP)

AHP was introduced by Saaty (1980) and is considered as a multi-criteria and multi-objective method, in this method, weights, which are decisions made are assigned based on the knowledge and experience of an expert. These weights are assigned in a form of pairwise relative comparison (Bathrelloset *al.* 2017; Papadakis and Karimalis 2017).

In the Analytical Hierarchy Process (AHP) the numerical value for each conditioning factor must be between 1 and 9 in the comparison matrix as represented in (table 1). In the matrix of this study, the conditioning factors for gully occurrence were organized hierarchically. A numerical value was allocated to each predisposing factor, based on their importance as compared with one another (Saaty 1980). The Eigenvalue (λ_{max}) and the Consistency Ratio (CR) were gotten after calculations were executed using the average of the hierarchically arranged factors according to Saaty (1980), in other to achieve a consistent comparison matrix the Eigenvalue (λ_{max}) and the total number of factors (n) have to be the same.

Mathematically Consistency Index is expressed as

$$CI = \frac{\lambda_{max} - n}{n - 1}$$

CI is the consistency index, λ_{max} is the Eigenvalue, and n represents the total number of factors being compared. Consistency Ratio (CR) is used to check for the consistency of the comparison matrix

CR is expressed as follows:

$$CR = \frac{CI}{RI}$$

CR represents the Consistency Ratio, CI represents the Consistency Index, and RI is the Random consistency Index of the pairwise comparison matrix. Table 2 shows the Random consistency index. The rule for the consistency index states that a Consistency Ratio (CR) that is equal to or less than 0.1 signifies that the matrix is acceptable; while a ratio of more than 0.1 means that the matrix is not consistent (Saaty 1980). The susceptibility index map was finally generated for the AHP model in the ArcGIS environment integrating the Arc Map raster calculator, the gully susceptibility index map generated was subsequently divided into low, moderate, high, and very high susceptibility zones according to the natural break classification method (Tian *et al.* 2017).

Gully erosion Inventory

To generate a comprehensive and dependable gully inventory map, as shown in Fig. 5, a detailed field survey was done, (Guzzetti *et al.* 2000) and more gullies were identified from high-resolution imagery from Google Earth. Fig.6 shows some photographs of some gullies in the study area. Next was the conversion of the gully areas represented as polygon to points and they were also overlain on a hill shade view of the area. Among all the 150 mapped gullies, 75% (113 gullies) of the mapped gullies in the study area were used for training. The training data was used in the modeling phases for the spatial prediction of gullies susceptible zones in the study area. While 25% (37 gullies) of the mapped gullies were used as testing data (Chung and Fabbri 2003; Dube *et al.* 2014) this was utilized in the validation of the gully erosion susceptibility models generated.

Conditioning factors

Quite a several factors contribute to gully erosion as discussed in the literature (Dube *et al.* 2014), the occurrence of gully erosion and its behavior depends on the following factors: topography characteristics, climate, lithology, soil characteristics, and land use (Poesen *et al.* 2003; Gutiérrez *et al.* 2009a.). The erodibility of the geologic formation in an area and the erosivity of surface runoff determine how susceptible the environment is to the formation of the gully (Conoscenti *et al.* 2008; Confortiet *al.* 2011)

Drainage buffer

The movement of eroded sediments is usually facilitated by drainage, therefore it could be said that gullies are associated with drainage (Conoscenti *et al.* 2014).The erosive actions in the drainage channels consequently reduce the shear strength of the slope material thereby increasing their chances of failure by sliding (Ozioko, O. H, Igwe, O. (2020).The distance from the drainage network was calculated in ArcGIS 10.4.1. Five buffer zones were created within the study area to determine the effect of drainages on gullies occurrence (Fig.7a), they include 0– 0.5km, 0.5– 1km, 1–2km, 2–3km, 3-5km.

Soil texture

Soil's physical properties are a major contributing factor to runoff, soil infiltration, gully occurrence, and soil resistance to erosion (Xia, D., *et al.* 2015).The occurrence of subsurface flow and piping is a function of the soil texture, the formation of gullies follows the collapse of the top of these pipes (Chaplot*et al.* 2005).It is expedient that the soil's texture is put into consideration in other to assess gully erosion susceptibility (Conoscenti *et al.* 2013). Four soil texture types were identified in the study areas (Fig.7b), they include sandy loam, stony, sandy clay, sandy,

Slope degree

ASTER DEM was used to obtain the slope information of the area the slope of the area was divided into five cases: 2-4,4-9, 9-16, 16-43(Fig.7c). Surface flow accumulation is common in flat areas and consequently initiation the formation of the

gully (Rahmati *et al.* 2015b; Ghorbani Nejad *et al.* 2017)

Land use

Through supervised classification, the landuse map (Fig.7d) was derived from Landsat 8™. Main landuse type in the study area include urban area, bare surface, shrubs and grasses, and farmlands. The stability of slope and gully occurrence is influenced by the landuse type (Zakerinejad and Maerker 2015). Infrastructural development such as roads, housing, and industries, prevents infiltration and increases the amount of surface runoff; this runoff concentrates and consequently produces gullies. Generally, bare surfaces and low vegetated areas are gully erosion-prone (Gutiérrez *et al.* 2009).

Elevation

The type of vegetation and the nature of precipitation are influenced by altitude. DEM was used to obtain the elevation of the area in the ArcGIS environment, five classes were obtained (Fig.7e): 330 - 414m, 414 - 477m, 477 - 544m, 544 - 611m, 611 - 721m

TWI

The topographic wetness index (TWI) which is a secondary topographic factor within the runoff model is usually employed to determine the extent to which topography control hydrological processes. TWI estimates the possibility of water accumulating in soil due to slope and upstream catchment area (Rahmati *et al.* 2016). Gómez-Gutiérrez *et al.* (2015), noted that TWI has to be considered in evaluating gully erosion susceptibility. TWI was derived from DEM. The TWI map was divided into four classes (Fig.7f), they include: < 7, 7.0 - 8.5, 8.5 - 10.6, >10.6

Lithology:

The lithological properties of the exposed geological formation affect the occurrence of gullies (Golestani *et al.* 2014). The geology thematic map (Fig.7g) represents the distribution of the gully erosion within the study area for the underlying lithology. The lithology thematic map was digitized from a geologic map produced by Nigeria Geological Survey Agency (NGSA) and was classified into four, according to the lithologic unit of the area; they include Kerri-Kerri Formation, Gombe Sandstone, Yolde Formation, and Pindiga Formation

Road buffer:

Paved roads effectively concentrate surface runoff. Road construction and expansion projects tend to encourage slope instability. Five classes of the road buffer map corresponding to buffer distances of 0-1km, 1-2km, 2-3km, 3-6km, 6-9km (Fig.7h).

Slope Aspect

The slope aspect has major control over the vegetation type because it influences the duration of sunlight. The slope aspect affects transpiration and moisture content also, evaporation, and indirectly affects the erosion process (Jaafari *et al.* 2014). Nine classes corresponding to flat, north, northeast, east, southeast, south, southwest, west and northwest are represented in the aspect map (Fig.7i)

Curvature:

Extensive analysis of profile curvature reveals useful geomorphological information (Davoodi Moghaddam *et al.* 2015). Three classes of the profile curvature (Fig.7j) include, convex, flat, and concave.

Results And Discussion

Prediction rate (frequency ratio)

The prediction rate result shows that drainage buffer, soil texture, slope degree, and landuse, have the major contribution to gully occurrence with a prediction rate of 4.21, 3.25, 2.49, 2.27, respectively as shown in (Table 13) Others include: elevation (2.03), TWI (1.79), Geology(1.68), Road buffer(1.64), Aspect(1.61), curvature (1).

Interpretation of Frequency ratio values for each factor class

The Frequency Ratio correlation value varies between <1 to >1 , when FR value is observed to be less than 1, it indicates a low correlation between gully location and each class of the predisposing factor, on the other hand, a higher correlation exists if the FR value is observed to be higher than 1 (Poudyal, *et al* 2010).

Analysis of result obtained from the drainage buffer shows that the 0-500m class has the highest correlation with FR of (1.87) (Table 3), others include 500m-1km(0.553), 1km-2km(0.038), therefore it can be deduced that the probability of gully occurrence decreases as the distance from drainage increases.

For the soil texture, the FR value of 2.29, was observed for the sandy clay class while other classes have FR value <1 (Table 4). There is a dominance of sand in all classes, which could be attributed to the high erodibility since sand has no cohesion. This finding is in agreement with Mbaya (2012) who stated that the dominance of the sand portion in Nigeria savanna soils has accelerated the occurrence of gully erosion. The high sand content of the soil also indicates that infiltration and percolation are high, thereby bringing about a piping phenomenon and ceiling collapse caused by subsurface flow, this is also in sync with the outcome of work done by Mbaya (2012). The presence of clay in the soil may have contributed to the formation of a gully since clay exhibits shrink and swell characteristics, this could result in the formation of cracks during the alternating warm and dry seasons. These cracks at the first sudden rainfall concentrate the runoff and therefore gully erosion is formed. This is similar to findings by McClosky *et al*, (2016)

Assessment of FR for the relationship between slope degree and gully occurrence reveals that slope degree class 0-2⁰ is the only class with FR value >1 , (1.25), indicating a high correlation. While slope degree greater than 2 all have FR value <1 (Table 5). Golestain *et al* (2014) proved that areas with gentle slope are susceptible to surface flow accumulation and gully erosion.

The landuse variable shows that urban class and farmland class have the FR value >1 (2.39, 1.31) respectively, while other classes have values less than 1, (Table 6). The high FR value in the urban class could be attributed to the infrastructural development such as roads, housing, industries, which have sealed the ground surface thereby preventing infiltration and increasing the amount of surface runoff, this runoff concentrates consequently forming gullies. This land-use type also deprives the soil of vegetation cover which is supposed to hold the soils together and prevent the direct impact of a raindrop on the soil. The high FR value owned by the farmland class could be attributed to agricultural activities such as plowing, compaction by farm machines and overgrazing, etc. which might have caused the soil to lose its structure and cohesiveness and becomes easily eroded.

Rainfall characteristics and vegetation are influenced by elevation (Gómez-Gutiérrez *et al*. 2015). The FR value for elevation indicates that altitude between 477-544 (FR=2.06), 544-611m (FR=1.75), and 414-477m (FR= 1.27) possess a strong correlation with gully occurrence (Table 7).

Analysis of the frequency ratio for TWI shows a strong correlation for factor class >10.6 and 8.5-10.6, both having FR value >1 (Table 8). It can be deduced that classes with high TWI value are pointers to gully occurrence. This result is in agreement with the finding of Rahmati *et al* (2016) and Dube *et al* (2014).

Assessment of geology shows that the Yolde with units of sandstone and shale and Kerri-Kerri Formation class consisting of sandstone, shale, and clay, have a major contribution with FR value of 1.68 and 1.26 respectively (Table 9). Pindiga formation and Gombe sandstone have FR value <1

Road buffer reveals that Factor class <1km and 1-2km have a strong correlation with gully occurrence, with FR value of 1.119 and 1.079. Table 10, while other classes have FR value less than 1. This suggests that the probability of gully occurrence decreases with distance from the road.

The result from aspect shows that the following classes have a strong relation with gully occurrence: flat face, east, southeast, and north with the following FR values 3.70, 1.68, 1.20, and 1.24, Table 11. Other classes have FR value less than 1

Analysis of the profile curvature reveals that the concave class has a major contribution to gully occurrence with FR of 1.45 Table 12. The flat class and convex class have values <1 indicating a very low correlation with FR value of 0.89 and 0.87 respectively.

Analytical Hierarchy Process (AHP)

The result of the AHP pairwise comparison shows that drainage buffer, soil texture, geology, and landcover have the highest contribution to gully formation with criteria weight 0.19, 0.18, 0.15, 0.09, respectively, others include slope (0.07), curvature (0.072), road buffer (0.0704), aspect (0.054) elevation (0.050), TWI (0.047) having the lowest impact on gully erosion respectively. (Table 14) and (Table 15)

Gully susceptibility maps

The respective weights from the Frequency ratio and AHP were multiplied by each predisposing factor map. This method was employed to produce the area's gully erosion susceptibility index map. The GESM shows a range of susceptibility to the study area. The produced susceptibility index maps for the frequency ratio and AHP models were reclassified into four zones according to the quantile classification scheme (Figure 8a and 8b). That is low, medium, high, and very high susceptibility zones (Youssef *et al.* 2015).

VALIDATION

Gully density distribution

Prediction rate curves coupled with gully density distribution within the susceptible areas were employed to check for the validity of the susceptibility map. Gully erosion density distribution for frequency ratio and AHP reveals that gullies are concentrated in the very high susceptibility class and it decreases as it gets to the low susceptibility class, density values for FR include: 0.729, 0.223, 0.097, 0.005 (Table 16), and AHP include: 0.74, 10.23, 0.10, 0.006. (Table 17). Gupta *et al.* (2008) stated in his work that the distribution of density decreases from the high susceptibility class to low class, which is in agreement with this study

The area under the curve (AUC)

To determine the accuracy of the Frequency ratio and AHP model applied, the (AUC) area under the curve was employed (Mohammady *et al.* 2012); AUC analysis is an efficient technique for evaluating the correctness of a test (Razandi *et al.* 2015). This curve indicates the accuracy and reliability of a predicting system. Rahmati; *et al.* (2016) classified the AUC

values as: 0.5–0.6, poor; 0.6–0.7, average; 0.7–0.8, good; 0.8–0.9, very good; and 0.9–1, excellent. For this study, the FR and AHP model gave AUC values of 0.73 and 0.72 respectively (fig.9). The outcome indicates that both models have high prediction accuracy with the Frequency ratio model slightly higher than the AHP model. Therefore the GESM produced using these models in this study area is reliable and can be used for land management and future planning

Conclusion

It is important to identify areas susceptible to gully erosion and to generate susceptibility maps. A comprehensive and dependable gully inventory map was successfully developed through detailed field surveys and from high-resolution Google Earth imagery. The spatial relationship between gully occurrences and its ten carefully selected causative factors which include: drainage buffer, soil texture, slope degree, land use, elevation, TWI, Lithology, Road buffer, and aspect were assessed using FR and AHP model, the FR model revealed that drainage buffer, soil texture, slope degree, and landuse, have the major contribution to gully occurrence and according to AHP model drainage buffer, soil texture, geology, and landcover are the most important contributors. These two methods were employed to generate two gully erosion susceptibility maps (GESM) for the study area. The GESM shows a range of susceptibility in the study area. The gully erosion susceptibility index maps generated from the FR and AHP models were reclassified into four zones according to the quantile classification scheme.

The performances of the models were subsequently validated using the AUC plot and gully density distribution. AUC values of 0.73 and 0.72 were obtained for FR and AHP models respectively. The obtained values indicated that both models have high prediction accuracy, though that of the FR is slightly higher than AHP. In addition to the AUC, the gully erosion density distribution for both methods revealed that gullies are concentrated in the very high susceptibility class and it decreases as it gets to the low susceptibility class, this outcome is as expected. The high accuracy obtained from AUC plots coupled with the alignment of the gully density distribution with the varying susceptibility classes proves that the GESM produced is reliable and accurate. The GESM produced shall be of enormous importance for town planners and decision-makers when there is a need for future infrastructural developments.

List Of Abbreviations

AUC, AHP,FR,GESM,TWI,DEM, NGSA

Declarations

Availability of data and material:

The datasets used and/or analyzed during the current study are available from the corresponding author on reasonable request.

Competing conflicts:

The authors declare that they have no competing interests

Funding:

Prof. Ogbonnaya Igwe

Authors' contribution: OI was involved in the field exercise and contributed to every step of the modeling and was a major contributor in writing the manuscript.

UIJ was involved in the field exercise and produced the conditioning factor maps, he was also a major contributor in writing the manuscript

OS was involved in the field exercise and tested the models using AUC, gully density distribution and contributed towards writing the manuscript

OO generated the susceptibility index map from the FR and AHP models, he was a major contributor in writing the manuscript. All authors read and approved the final manuscript.

Acknowledgment: Thanks to staff and students of the Geology Department, University of Nigeria Nsukka.

References

1. Abedini, M., Ghasemyan, B., & Mogaddam, M. R. (2017). Landslide susceptibility mapping in Bijar city, Kurdistan Province, Iran: a comparative study by logistic regression and AHP models. *Environmental Earth Sciences*, 76(8), 308.
2. Abubakar, M. B., Dike, E. F. C., Obaje, N. G., Wehner, H., & Jauro, A. (2008). Petroleum prospectivity of Cretaceous Formations in the Gongola Basin, Upper Benue Trough, Nigeria: an organic geochemical perspective on a migrated oil controversy. *Journal of Petroleum Geology*, 31(4), 387-407.
3. Arabameri, A., Rezaei, K., Pourghasemi, H. R., Lee, S., & Yamani, M. (2018). GIS-based gully erosion susceptibility mapping: a comparison among three data-driven models and AHP knowledge-based technique. *Environmental earth sciences*, 77(17), 628.
4. Arabi, A. S., Nur, A., & Dewu, B. B. M. (2009). Hydro geo-electrical investigation in Gombe town and environs, northeastern Nigeria. *Journal of Applied Sciences and Environmental Management*, 13(3).
5. Bathrellos, G. D., Skilodimou, H. D., Chousianitis, K., Youssef, A. M., & Pradhan, B. (2017). Suitability estimation for urban development using multi-hazard assessment map. *Science of the total environment*, 575, 119-134.
6. Carter, J. D. (1963). The geology of parts of Adamawa, Bauchi and Bornu provinces in northeastern Nigeria. *Geological Survey of Nigeria Bulletin*, 30.
7. Chung, C. J. F., & Fabbri, A. G. (2003). Validation of spatial prediction models for landslide hazard mapping. *Natural Hazards*, 30(3), 451-472.
8. Chaplot, V., Giboire, G., Marchand, P., & Valentin, C. (2005). Dynamic modelling for linear erosion initiation and development under climate and land-use changes in northern Laos. *Catena*, 63(2-3), 318-328.
9. Conforti, M., Aucelli, P. P., Robustelli, G., & Scarciglia, F. (2011). Geomorphology and GIS analysis for mapping gully erosion susceptibility in the Turbolo stream catchment (Northern Calabria, Italy). *Natural hazards*, 56(3), 881-898.
10. Conoscenti, C., Agnesi, V., Angileri, S., Cappadonia, C., Rotigliano, E., & Märker, M. (2013). A GIS-based approach for gully erosion susceptibility modelling: a test in Sicily, Italy. *Environmental earth sciences*, 70(3), 1179-1195.
11. Conoscenti, C., Angileri, S., Cappadonia, C., Rotigliano, E., Agnesi, V., & Märker, M. (2014). Gully erosion susceptibility assessment by means of GIS-based logistic regression: a case of Sicily (Italy). *Geomorphology*, 204, 399-411.
12. Conoscenti, C., Di Maggio, C., & Rotigliano, E. (2008). GIS analysis to assess landslide susceptibility in a fluvial basin of NW Sicily (Italy). *Geomorphology*, 94(3-4), 325-339.
13. Dube, F., Nhapi, I., Murwira, A., Gumindoga, W., Goldin, J., & Mashauri, D. A. (2014). Potential of weight of evidence modeling for gully erosion hazard assessment in Mbire District–Zimbabwe. *Physics and Chemistry of the Earth, Parts A/B/C*, 67, 145-152.
14. Ghorbani Nejad, S., Falah, F., Daneshfar, M., Haghizadeh, A., & Rahmati, O. (2017). Delineation of groundwater potential zones using remote sensing and GIS-based data-driven models. *Geocarto international*, 32(2), 167-187.
15. Golestani, G., Issazadeh, L., & Serajamani, R. (2014). Lithology effects on gully erosion in Ghoorichay Watershed using RS & GIS. *Int J Biosci*, 4(2), 71-76.

16. Gómez-Gutiérrez, Á., Conoscenti, C., Angileri, S. E., Rotigliano, E., & Schnabel, S. (2015). Using topographical attributes to evaluate gully erosion proneness (susceptibility) in two mediterranean basins: advantages and limitations. *Natural Hazards*, 79(1), 291-314.
17. Gupta, R. P., Kanungo, D. P., Arora, M. K., & Sarkar, S. (2008). Approaches for comparative evaluation of raster GIS-based landslide susceptibility zonation maps. *International Journal of Applied Earth Observation and Geoinformation*, 10, 330–341. <https://doi.org/10.1016/j.jag.2008.01.003>
18. Gutiérrez, Á. G., Schnabel, S., & Contador, F. L. (2009). Gully erosion, land use and topographical thresholds during the last 60 years in a small rangeland catchment in SW Spain. *Land Degradation & Development*, 20(5), 535-550.
19. Guzzetti, F., Cardinali, M., Reichenbach, P., & Carrara, A. (2000). Comparing Landslide Maps: A Case Study in the Upper Tiber River Basin, Central Italy. *Environmental management*, 25(3).
20. Jaafari, A., Najafi, A., Pourghasemi, H. R., Rezaeian, J., & Sattarian, A. (2014). GIS-based frequency ratio and index of entropy models for landslide susceptibility assessment in the Caspian forest, northern Iran. *International Journal of Environmental Science and Technology*, 11(4), 909-926.
21. Kirkby, M. J., & Bracken, L. J. (2009). Gully processes and gully dynamics. *Earth Surface Processes and Landforms: The Journal of the British Geomorphological Research Group*, 34(14), 1841-1851.
22. Lee, S., & Talib, J. A. (2005). Probabilistic landslide susceptibility and factor effect analysis. *Environmental Geology*, 47(7), 982-990.
23. Ligonja, P. J., & Shrestha, R. P. (2015). Soil erosion assessment in kondoia eroded area in Tanzania using universal soil loss equation, geographic information systems and socioeconomic approach. *Land Degradation & Development*, 26(4), 367-379.
24. Magliulo, P. (2012). Assessing the susceptibility to water-induced soil erosion using a geomorphological, bivariate statistics-based approach. *Environmental earth sciences*, 67(6), 1801-1820.
25. Mbaya, L. A. (2017). Spatial analysis of gully erosion control measures in Gombe town, Gombe state Nigeria. *Advances in Image and Video Processing*, 5(4), 17-17.
26. Mbaya, L. A., Ayuba, H. K., & Abdullahi, J. (2012). An Assessment of Gully Erosion in Gombe Town, Gombe State, Nigeria. *Journal of Geography and Geology*, 4(3), 110.
27. McCloskey, G. L., Wasson, R. J., Boggs, G. S., & Douglas, M. (2016). Timing and causes of gully erosion in the riparian zone of the semi-arid tropical Victoria River, Australia: Management implications. *Geomorphology*, 266, 96-104.
28. Moghaddam, D. D., Rezaei, M., Pourghasemi, H. R., Pourtaghie, Z. S., & Pradhan, B. (2015). Groundwater spring potential mapping using bivariate statistical model and GIS in the Taleghan watershed, Iran. *Arabian Journal of Geosciences*, 8(2), 913-929.
29. Nampak, H., Pradhan, B., Mojaddadi Rizeei, H., & Park, H. J. (2018). Assessment of land cover and land use change impact on soil loss in a tropical catchment by using multitemporal SPOT-5 satellite images and Revised Universal Soil Loss Equation model. *Land degradation & development*, 29(10), 3440-3455.
30. Oh, H. J., Lee, S., & Hong, S. M. (2017). Landslide susceptibility assessment using frequency ratio technique with iterative random sampling. *Journal of Sensors*, 2017.
31. Orazulike, D. M. (1987). Recent cracks in the vicinity of Pindiga, Bauchi State: Product of groundwater solution. *Nigerian J. Mining Geol*, 23
32. Ouyang, C., Zhou, K., Xu, Q., Yin, J., Peng, D., Wang, D., & Li, W. (2017). Dynamic analysis and numerical modeling of the 2015 catastrophic landslide of the construction waste landfill at Guangming, Shenzhen, China. *Landslides*, 14(2), 705-

33. Ozioko, O. H., & Igwe, O. (2020). GIS-based landslide susceptibility mapping using heuristic and bivariate statistical methods for Iva Valley and environs Southeast Nigeria. *Environmental Monitoring and Assessment*, 192(2), 1-19.
34. Papadakis, M., & Karimalis, A. (2017). Producing a landslide susceptibility map through the use of analytic hierarchical process in finikas watershed, North Peloponnese, Greece. *Am J Geogr Inf Syst*, 6(1A), 14-22.
35. Pearson, M. J., & Obaje, N. G. (1999). Onocerane and other triterpenoids in Late Cretaceous sediments from the Upper Benue Trough, Nigeria: tectonic and palaeoenvironmental implications. *Organic Geochemistry*, 30(7), 583-592.
36. Poesen, J., Nachtergaele, J., Verstraeten, G., & Valentin, C. (2003). Gully erosion and environmental change: importance and research needs. *Catena*, 50(2-4), 91-133.
37. Poudyal, C. P., Chang, C., Oh, H. J., & Lee, S. (2010). Landslide susceptibility maps comparing frequency ratio and artificial neural networks: a case study from the Nepal Himalaya. *Environmental Earth Sciences*, 61(5), 1049-1064.
38. Rahmati, O., Samani, A. N., Mahdavi, M., Pourghasemi, H. R., & Zeinivand, H. (2015). Groundwater potential mapping at Kurdistan region of Iran using analytic hierarchy process and GIS. *Arabian Journal of Geosciences*, 8(9), 7059-7071.
39. Rahmati, O., Pourghasemi, H. R., & Melesse, A. M. (2016). Application of GIS-based data driven random forest and maximum entropy models for groundwater potential mapping: a case study at Mehran Region, Iran. *Catena*, 137, 360-372.
40. Rahmati, O., Tahmasebipour, N., Haghizadeh, A., Pourghasemi, H. R., & Feizizadeh, B. (2017). Evaluation of different machine learning models for predicting and mapping the susceptibility of gully erosion. *Geomorphology*, 298, 118-137.
41. Razandi, Y., Pourghasemi, H. R., Neisani, N. S., & Rahmati, O. (2015). Application of analytical hierarchy process, frequency ratio, and certainty factor models for groundwater potential mapping using GIS. *Earth Science Informatics*, 8(4), 867-883.
42. Rizeei, H. M., Saharkhiz, M. A., Pradhan, B., & Ahmad, N. (2016). Soil erosion prediction based on land cover dynamics at the Semenyih watershed in Malaysia using LTM and USLE models. *Geocarto international*, 31(10), 1158-1177.
43. Saaty, T.L. (1980). *The analytical hierarchy process. PrioritySetting*. MacGraw-Hill: Resource Allocation, New York International Book Company 287.
44. Tian, Y., Xu, C., Chen, J., & Hong, H. (2017). Spatial distribution and susceptibility analyses of pre-earthquake and coseismic landslides related to the Ms 6.5 earthquake of 2014 in Ludian, Yunan, China. *Geocarto International*, 32(9), 978-989.
45. Torri, D., Borselli, L., Gariano, S. L., Greco, R., laquinta, P., Iovine, G., ... & Terranova, O. G. (2012). Identifying gullies in the Mediterranean environment by coupling a complex threshold model and a GIS. *RENDICONTI Online della Società Geologica Italiana*, 89(PART 1), 441-443.
46. Valentin, C., Poesen, J., & Li, Y. (2005). Gully erosion: impacts, factors and control. *Catena*, 63(2-3), 132-153.
47. Xia, D., Deng, Y., Wang, S., Ding, S., & Cai, C. (2015). Fractal features of soil particle-size distribution of different weathering profiles of the collapsing gullies in the hilly granitic region, south China. *Natural Hazards*, 79(1), 455-478.
48. Zaborski, P., Ugodulunwa, F., Idornigie, A., Nnabo, P., & Ibe, K. (1997). Stratigraphy and structure of the Cretaceous Gongola Basin, northeast Nigeria. *Bulletin des Centres de Recherches Exploration-Production Elf Aquitaine*, 21(1), 153-185.
49. Zakerinejad, R., & Maerker, M. (2015). An integrated assessment of soil erosion dynamics with special emphasis on gully erosion in the Mazayjan basin, southwestern Iran. *Natural Hazards*, 79(1), 25-50.

Tables

Table.1: The scale of preference between two factors in AHP (Saaty 1980)

Preference factor	Degree of preference	Definition
1	Equally	two factors have equal importance to the desired objective
3	Moderately	One factor slightly has more importance than the other to the desired objective
5	Strongly	A factor strongly has higher importance than the other towards achieving the desired objective
7	Very strongly	Here a factor has very strong importance more than the other towards achieving its objective
9	Extremely	One factor is extremely more important than the other toward achieving the desired objective
2,4,6,8	Intermediate	when factor importance is between 1,3,4,7 and 9

Table 2: Random index (Saaty 1980)

No.	1	2	3	4	5	6	7	8	9	10
CR	0.00	0.00	0.58	0.90	1.12	1.24	1.32	1.41	1.45	1.49

Table 3: Showing FR values for drainage buffer classes

Factor	Factor class	No. of points	% of points	class area	% of class area	Frequency ratio	Relative frequency
Drainage buffer	<500M	89127.17	83.18	257741	44.47	1.87	0.75
	500m-1KM	17066.91	15.92	166659	28.75	0.55	0.22
	1KM-2KM	948.16	0.88	133386	23.01	0.03	0.01
	2KM-3KM	0		18938	3.26	0	0
	3KM-5KM	0		2859	0.49	0	0
	Sum		107142.2	100	579800	100	2.46

Table 4: Showing FR values for soil texture classes

Soil texture	factor classes	No. of points	% of points	class area	% of class area	Frequency ratio	Relative frequency
	sandy loam	40770.94	38.05	295312	50.94	0.74	0.19
	Stony	0	0	9047	1.56	0	0
	Sandy clay	36030.13	33.62	85107	14.68	2.29	0.58
	Sandy	30341.17	28.31	190248	32.81	0.86	0.22
	sum	107142.2	100	579800	100	3.90	1

Table 5: Showing FR values for slope classes

Slope	Factor classes	No. of points	% of points	Class area	%of class area	Frequency ratio	Relative frequency
	0-2	65423.14	61.06	283093	48.82	1.25	0.44
	2-4	34133.81	31.85	217715	37.54	0.84	0.30
	4-9	7585.291	7.07	59650	10.28	0.68	0.24
	9-16	0	0	14653	2.52	0	0
	16-43	0	0	4708	0.81	0	0
	Sum	107142.2	100	579819	100	2.78	1

Table 6: Showing FR values for landuse classes

Landuse	factor classes	No. of points	% of points	class area	% of class area	Frequency ratio	Relative frequency
	Urban area	29393	27.43	66507	11.47	2.39	0.48
	BARESURFACE	7585.291	7.07	110674	19.08	0.37	0.07
	SHRUBS & GRASSES	51200.72	47.78	324531	55.97	0.85	0.17
	FARMLANDS	18963.23	17.69	78107	13.47	1.31	0.26
	sum	107142.2	100	579819	100	4.93	1

Table 7: Showing FR values for elevation classes

Elevation	factor classes	No. of points	% of points	class area	% of class area	Frequency ratio	Relative frequency
	330 –414m	28444.84	26.54	149566	48.82	0.54	0.09
	414 –477m	51200.72	47.78	156698	37.54	1.27	0.22
	477 –544m	22755.87	21.23	104788	10.28	2.06	0.36
	544 –611m	4740.807	4.42	105167	2.52	1.75	0.31
	611 –721m	0	0	63600	0.81	0	0
	sum	107142.2	100	579819	100	5.63	1

TWI	factor classes	No. of points	% of points	class area	% of class area	Frequency ratio	Relative frequency
	< 7.0	36030.13	33.62	250191	43.14	0.77	0.14
	7.0 - 8.5	38874.62	36.28	213435	36.81	0.98	0.18
	8.5 - 10.6	15170.58	14.15	79075	13.63	1.03	0.19
	>10.6	17066.91	15.92	37118	6.40	2.48	0.47
	Sum	107142.2	100	579819	100	5.29	1

Table 8: Showing FR values for TWI classes

Geology	factor classes	No. of points	% of points	class area	% of class area	Frequency ratio	Relative frequency
	kerri kerri form	81541.88	76.10	349006	60.20	1.26	0.34
	Gombe sandstone	12326.1	11.50	111965	19.31	0.59	0.16
	Yolde formation	12326.098	11.50	83748	14.44	1.68	0.45
	Pindiga formation	948.1614	0.88	35002	6.03	0.14	0.03
	sum	107142.2	100	579721	100	3.69	1

Table 9: Showing FR values for geology classes

Road buffer	factor classes	No. of points	% of points	class area	% of class area	Frequency ratio	Relative frequency
	>1KM	50252.56	46.90	242971	41.88	1.11	0.29
	1-2KM	29393	27.43	147361	25.40	1.07	0.28
	2-3KM	14222.42	13.27	97078	16.73	0.79	0.21
	3-6KM	13274.26	12.38	92341	15.92	0.77	0.20
	6-9KM	0	0	275	0.04	0	0
	sum	107142.2	100	580026	100	3.77	1

Table 10: Showing FR values for road buffer classes

Table 11: Showing FR values for aspect classes

Aspect	factor classes	No. of points	% of points	class area	% of class area	Frequency ratio	Relative frequency
	Flat	1896.323	1.76	2770	0.47	3.70	0.30
	North	6637.13	6.19	44532	7.68	0.80	0.06
	North East	14222.42	13.27	85699	14.78	0.89	0.07
	East	29393	27.43	94206	16.24	1.68	0.13
	South East	19911.39	18.58	89357	15.41	1.20	0.09
	South	12326.1	11.50	68307	11.78	0.97	0.08
	South West	5688.969	5.30	51571	8.89	0.59	0.04
	West	1896.323	1.76	52901	9.12	0.19	0.01
	North West	8533.453	7.96	61720	10.64	0.74	0.06
	North	6637.13	6.19	28756	4.95	1.24	0.10

Table 12: Showing FR values for curvature

Factor	factor classes	No. of points	% of points	class area	% of class area	Frequency ratio	Relative frequency
Curvature	Convex	17066.91	15.92	105704	18.23	0.87	0.27
	Flat	59734.17	55.75	361217	62.29	0.89	0.27
	Concave	30341.17	28.31	112898	19.47	1.45	0.45
	Sum	107142.2	100	579819	100	3.22	1

Table 13. Prediction rate as derived from frequency ratio

Conditioning factors	min RF	max RF	(max-min)	min tot.	Prediction rate
Profile curvature	0.27	0.45	0.18	0.18	1
Aspect	0.01	0.30	0.29	0.18	1.61
Road buffer	0	0.29	0.29	0.18	1.64
Geology	0.03	0.34	0.30	0.18	1.68
TWI	0.14	0.47	0.32	0.18	1.79
Elevation	0	0.36	0.36	0.18	2.03
Landuse	0.07	0.48	0.40	0.18	2.27
Slope	0	0.44	0.44	0.18	2.49
Soil texture	0	0.58	0.58	0.18	3.25
Drainage buffer	0	0.75	0.75	0.18	4.21

Table 14: Final criteria weights of factors from AHP

Variables	Criteria weight	Integer weight
TWI	0.047	4.77
Elevation	0.050	5.00
Aspect	0.054	5.49
Road buffer	0.070	7.04
Curvature	0.072	7.26
Slope	0.075	7.58
Land cover	0.096	9.61
Geology	0.152	15.24
Soil	0.180	18.08
drainage buffer	0.198	19.887

Table15: AHP comparison matrix for the conditioning factors

AHP Matrix										
Predictors	Aspect	Road buffer	TWI	Drainage buffer	Landcover	Slope	Geology	Curvature	Elevation	Soil
Aspect	1	1	1	1/3	1/2	1/2	1/3	1	2	1/4
Road buffer	1	1	2	1/3	1/2	1	1/2	1	3	1/3
TWI	1	1/2	1	1/4	1/2	1/2	1/3	1	1	1/3
drainage buffer	3	3	4	1	2	3	2	3	5	1
Land cover	2	2	2	1/2	1	2	1/2	1/2	3	1/2
Slope	2	1	2	1/3	1/2	1	1/2	1	3	1/3
Geology	3	2	3	1/2	2	2	1	3	4	1
Curvature	1	1	1	1/3	2	1	1/3	1	2	1/3
Elevation	1/2	1/3	1	1/5	1/3	3	1/4	1/2	1	1/4
Soil	4	3	3	1	2	3	1	3	4	1
Sum	18.50	14.83	20.00	4.78	11.33	17.00	6.75	15.00	28.00	5.33
CR= 0.064										

Table16: Gully density distribution for FR

Class	area (m ²)	%(class)	class area (km ²)	gully area (km ²)	Gully density
Low	165010	28.67121	0.16501	0.0009	0.005
Medium	146509	25.45658	0.146509	0.014	0.097
High	199041	34.58425	0.199041	0.044	0.223
very high	64965	11.28795	0.064965	0.047	0.729

Table 17: Gully density distribution for AHP

Class	area (m ²)	%(class)	gully area (km ²)	gully area (km ²)	gully density
Low	155010	28.46	0.15501	0.0009	0.006
Medium	136509	25.06	0.136509	0.014	0.104
High	189041	34.71	0.189041	0.044	0.235
very high	63965	11.74	0.063965	0.047	0.741

Figures

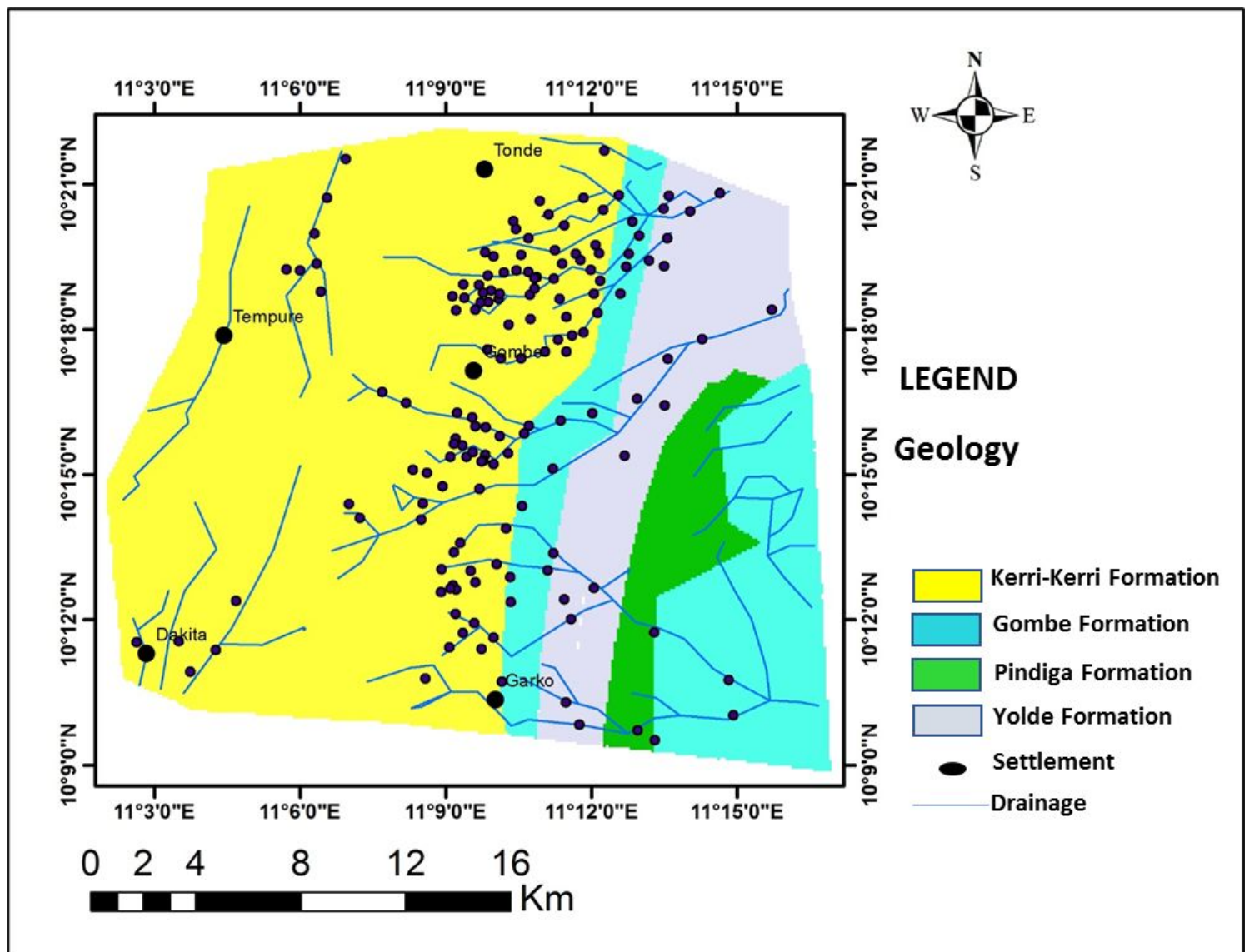


Figure 1

Location and accessibility map of the study area

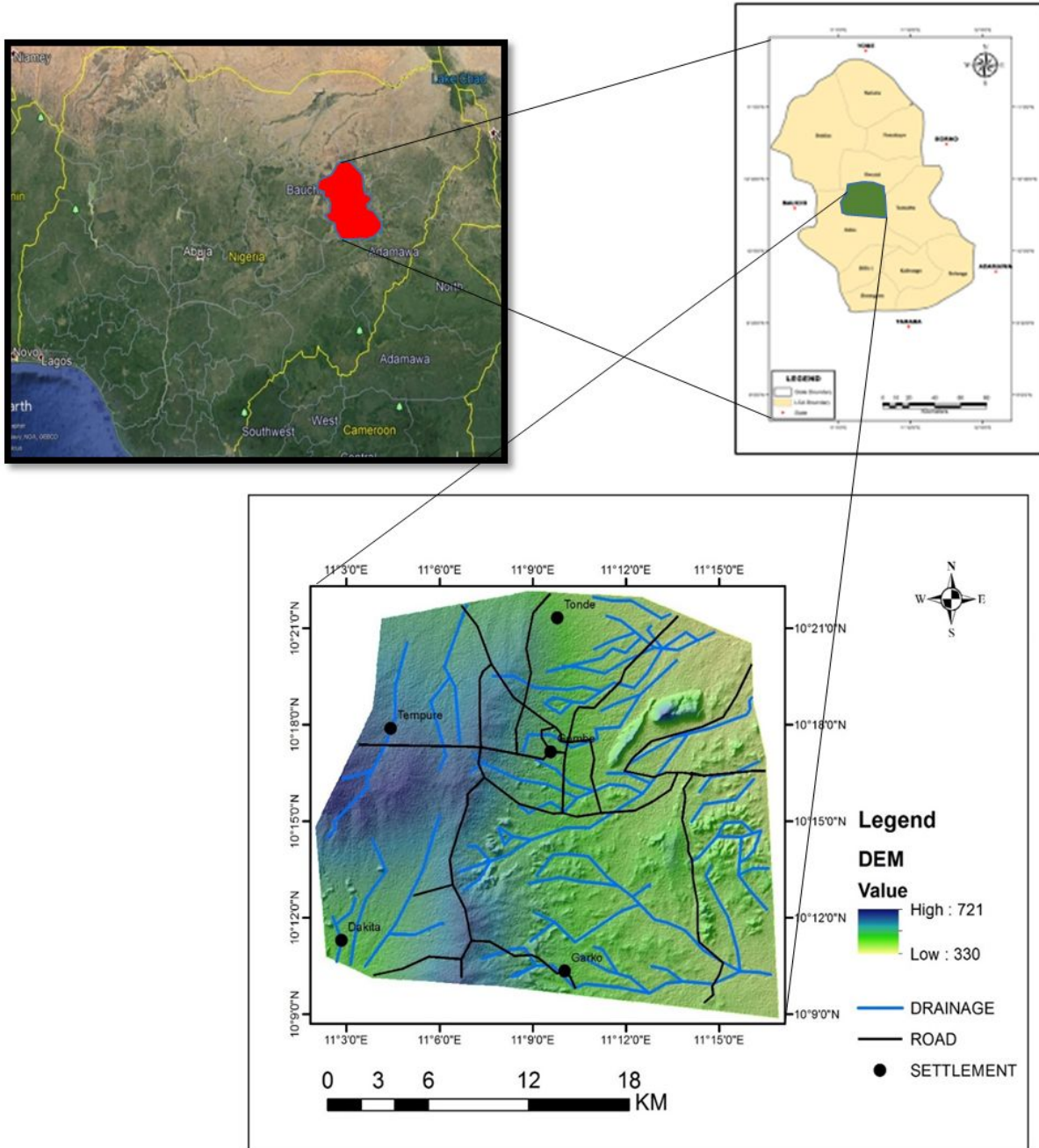


Figure 2

Geologic map of the study area

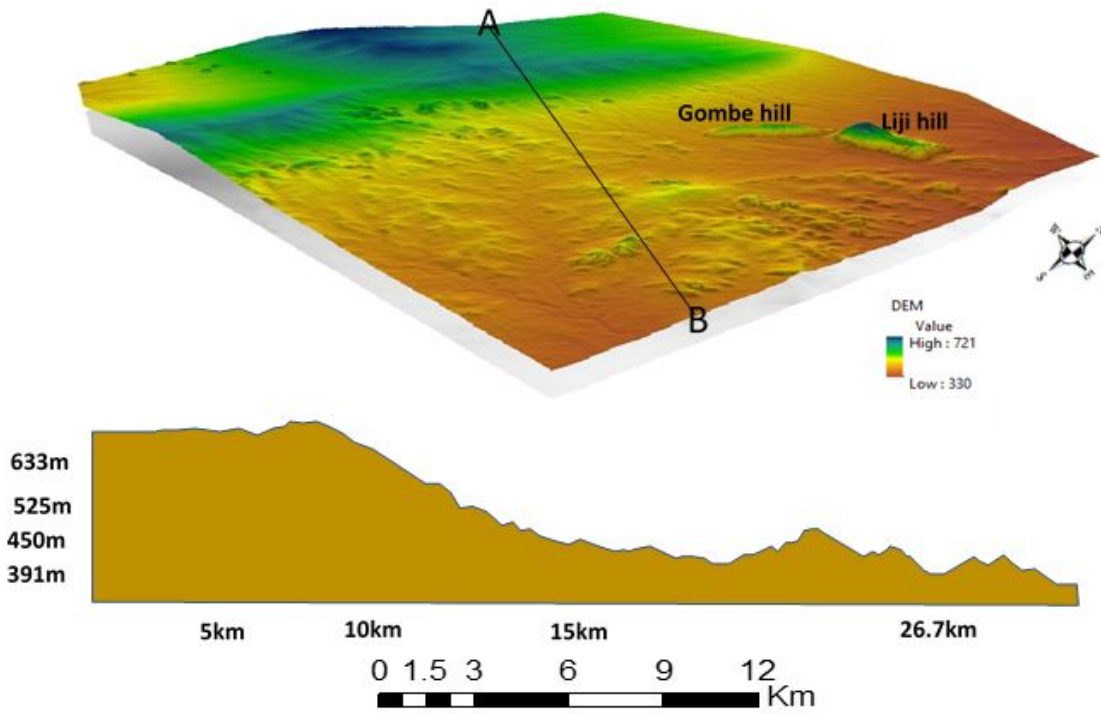


Figure 3

3D Dem and topographical profile of the study area

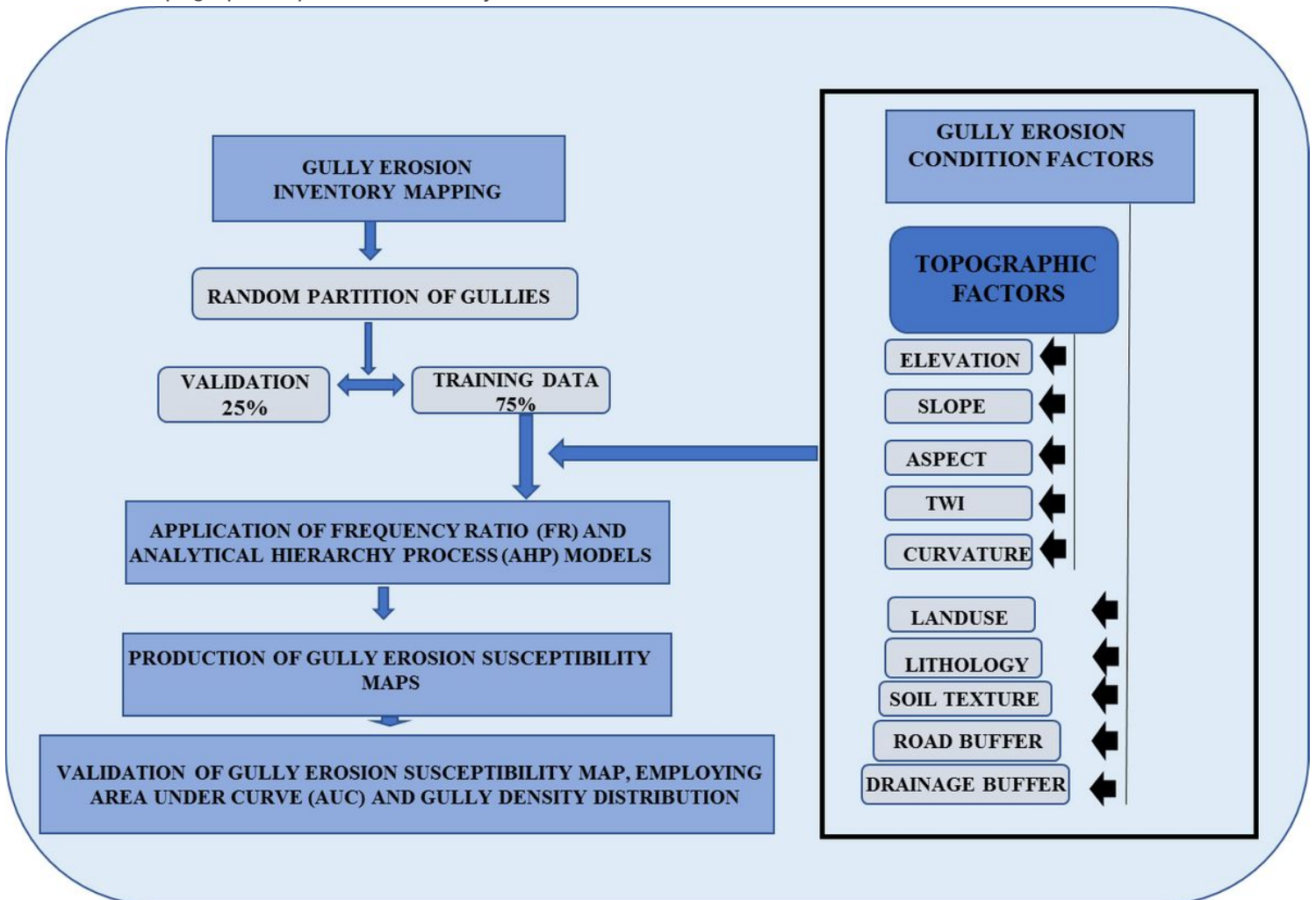


Figure 4

Methodology flowchart

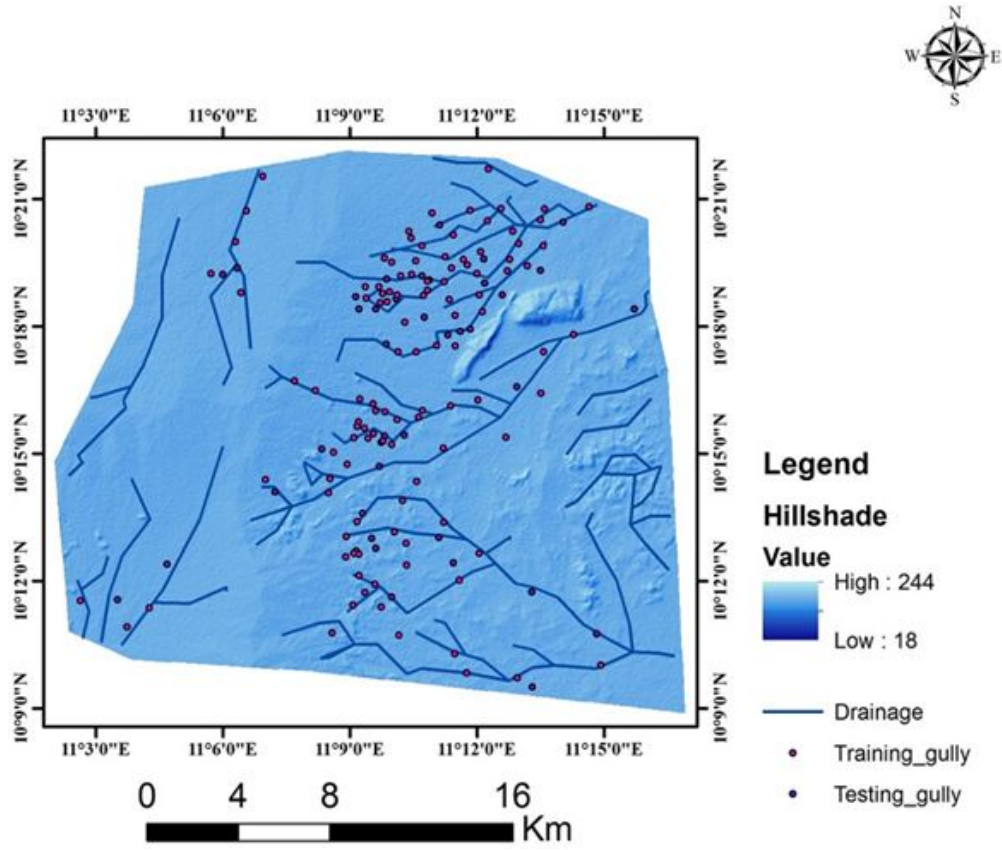


Figure 5

Gully inventory map shown as hill shade view of the area



Figure 6

Field photograph of some gullies in the study area

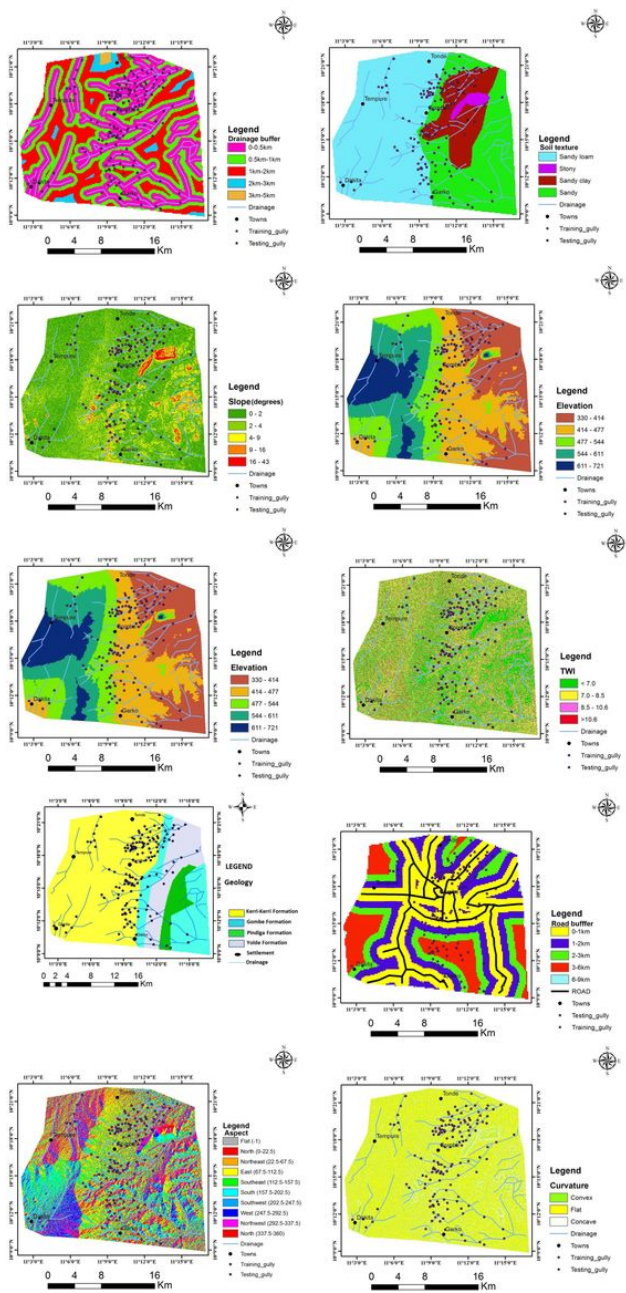


Figure 7

Thematic maps of the selected conditioning factors

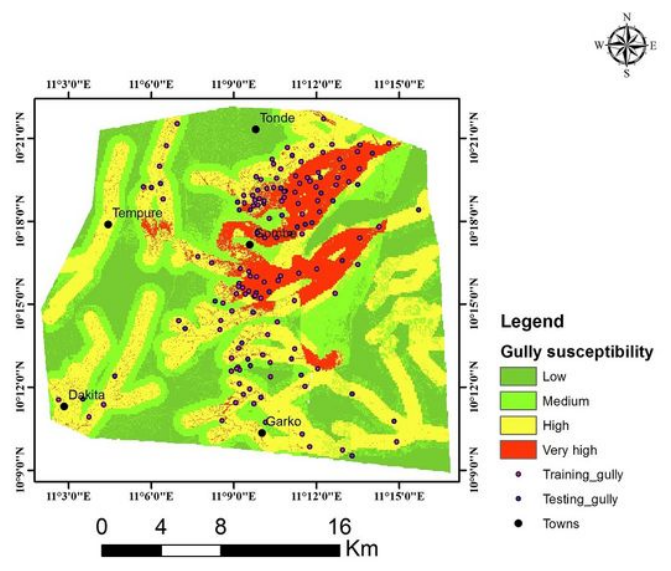
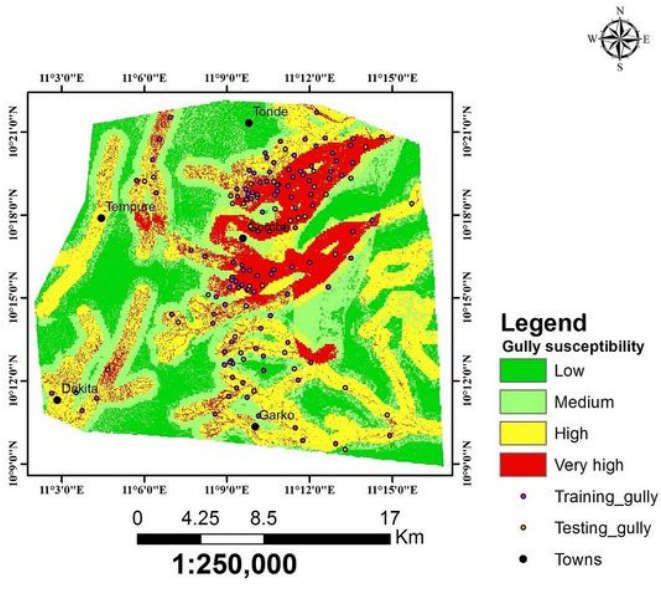


Figure 8

Gully erosion susceptibility maps for FR (A) and AHP(B)model

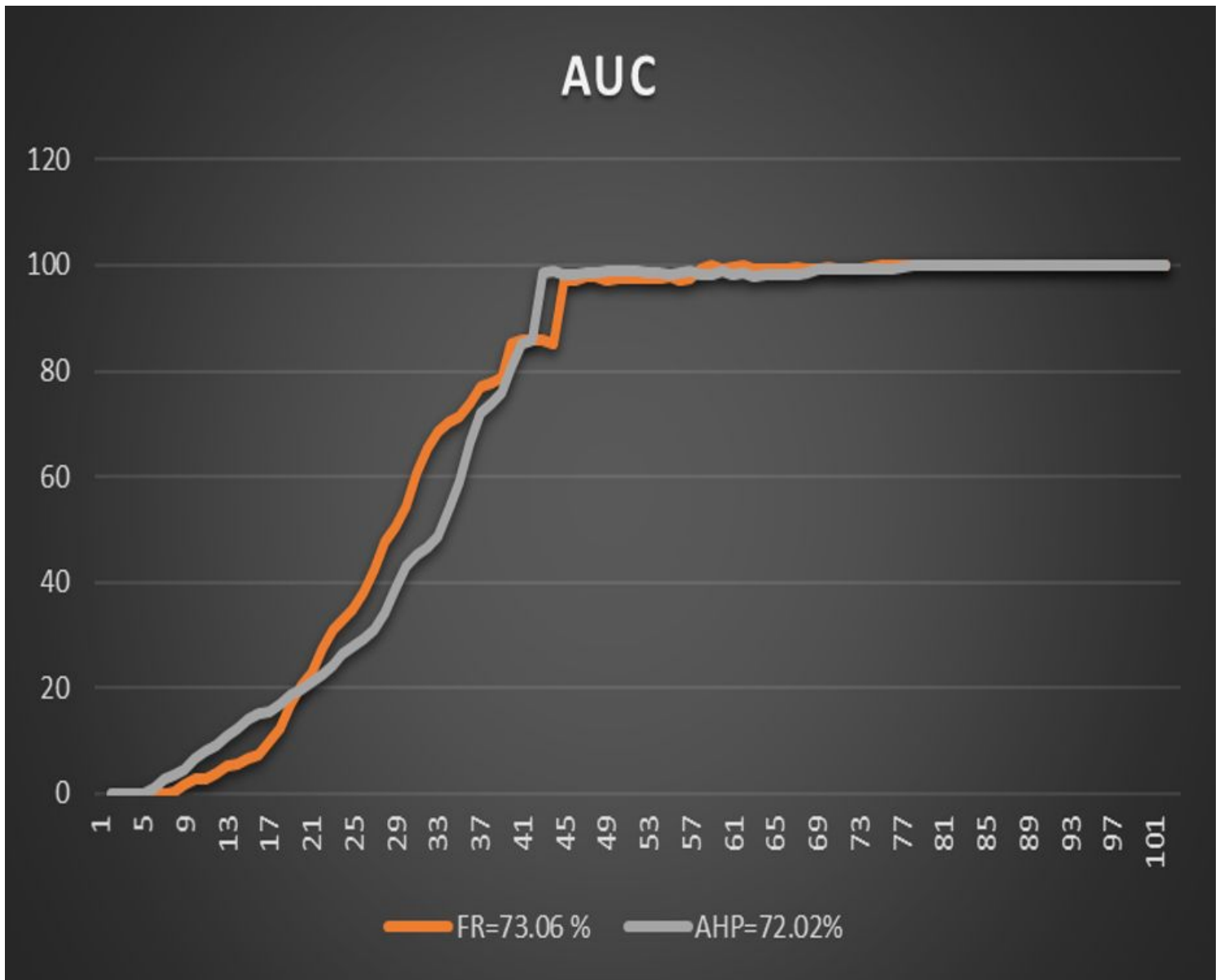


Figure 9

Area under curve plot showing the predictive capacity of the two models